

Published in final edited form as:

Nat Struct Mol Biol. 2009 October ; 16(10): 1016–1020. doi:10.1038/nsmb.1675.

LIN-28 and the poly(U) polymerase PUP-2 regulate *let-7* microRNA processing in *Caenorhabditis elegans*

Nicolas J. Lehrbach^{1,2,*}, Javier Armisen^{1,2,*}, Helen L. Lightfoot^{1,3}, Kenneth J. Murfitt¹, Anthony Bugaut³, Shankar Balasubramanian³, and Eric A. Miska^{1,2}

¹Wellcome Trust Cancer Research UK Gurdon Institute, University of Cambridge, The Henry Wellcome Building of Cancer and Developmental Biology, Tennis Court Rd, Cambridge CB2 1QN, UK

²Department of Biochemistry, University of Cambridge, Tennis Court Rd, Cambridge CB2 1GA, UK

³Department of Chemistry, University of Cambridge, Lensfield Rd, Cambridge CB2 1EW, UK

Abstract

The *let-7* microRNA (miRNA) is an ultraconserved regulator of stem cell differentiation and developmental timing, and a candidate tumour suppressor. Here we show that LIN-28 and the poly(U) polymerase PUP-2 regulate *let-7* processing in *C. elegans*. We demonstrate that *lin-28* is necessary and sufficient to block *let-7* activity *in vivo*; LIN-28 directly binds *let-7* pre-miRNA to prevent Dicer processing. Moreover, we have identified a poly(U) polymerase, PUP-2, which regulates the stability of LIN-28 blockaded *let-7* pre-miRNA, and contributes to *lin-28* dependent regulation of *let-7* during development. We show that PUP-2 and LIN-28 interact directly, and that LIN-28 stimulates uridylation of *let-7* pre-miRNA by PUP-2 *in vitro*. Our results demonstrate that LIN-28 and *let-7* form an ancient regulatory switch, conserved from nematodes to humans, and provide insight into the mechanism of LIN-28 action *in vivo*. Uridylation by a PUP-2 orthologue might regulate *let-7* and additional miRNAs in other species. Given the roles of Lin28 and *let-7* in stem cell and cancer biology, we propose such poly(U) polymerases are potential therapeutic targets.

Small RNAs regulate gene expression in many eukaryotes including plants, animals and fungi. miRNAs are endogenous short RNAs that modulate gene expression by blocking translation and/or destabilizing target mRNAs^{1,2}. In animals miRNAs are transcribed as long precursors (pri-miRNAs), which are processed in the nucleus by the RNase III enzyme complex Drosha-Pasha/DGCR8 to form ~80 nt pre-miRNAs, or are derived directly from introns³. pre-miRNAs are exported from the nucleus and processed by the RNase III enzyme Dicer, and incorporated into an Argonaute-containing RNA-induced silencing complex (RISC). The first identified miRNAs, the products of the *C. elegans* genes *lin-4* and *let-7*, control cell fates during larval development⁴. When either *lin-4* or *let-7* is inactivated, specific epithelial cells fail to differentiate and undergo additional divisions. *lin-4* acts during early larval development, regulating *lin-14* and *lin-28* mRNAs^{4,5,6,7,8}. *let-7* acts during late larval development, regulating *lin-41*, *hbl-1*, *daf-12* and *pha-4* mRNAs^{9,10,11,12}. As such, the time of appearance of these miRNAs must be tightly controlled. In *C. elegans*

Correspondence and requests for materials should be addressed to E.A.M. (eam29@cam.ac.uk).

*These authors contributed equally.

Author information N.J.L., S.B. and E.A.M. conceived the original project. N.J.L. carried out all experiments unless stated otherwise. J.A. carried out northern blotting, uridylyase assays and microarray experiments. H.L.L., J.A., A.B. carried out RNA mobility shift assays. K.J.M., J.A. carried out some of the *in vitro* binding assays. N.J.L., J.A. and E.A.M. wrote the manuscript.

and other animals the expression of *let-7* is developmentally regulated, but the mechanisms underlying this regulation remain unknown¹³. Post-transcriptional regulation of specific miRNAs has recently been uncovered¹⁴. *let-7* biogenesis is blocked by Lin28 at either the Drosha^{15,16} or Dicer^{17,18} step in mammalian cell culture. Lin28 is a conserved RNA-binding protein, which in mammals controls stem cell lineages and inhibits *let-7* miRNA processing *in vitro*^{15,16,17,18,19}. However, the mechanism and *in vivo* significance of this activity are unclear.

RESULTS

An *in vivo* assay of *let-7* miRNA function reveals developmental regulation

To study the mechanism of miRNA action *in vivo*, we established a quantitative miRNA reporter assay based on *let-7* in *C. elegans* (Fig 1a,b and Supplementary Methods). We generated two transgenes comprising the promoter of *myo-2*, the coding sequences of either GFP or mCherry and the 3'UTR of either *lin-41* or *unc-54* (*myo-2::gfp::lin-41* and *myo-2::mcherry::unc-54*; hereafter referred to as the *let-7 sensor*; Fig. 1a). The *myo-2* promoter confers expression exclusively in the pharyngeal muscle, the food pump of *C. elegans*²⁰, and *lin-41* is a genetically identified target of the *let-7* miRNA⁹, whereas the *unc-54* 3'UTR is not known to be regulated by any miRNA. Transgenic animals carrying an intrachromosomal array of the *let-7 sensor* expressed both GFP and mCherry strongly throughout larval development (Fig. 1c). As expected, a transgene expressing *let-7* (*myo-2::let-7*) silenced GFP, but not mCherry (Fig. 1d). Surprisingly, this effect was developmentally regulated; inhibition of GFP is markedly stronger in adults than L1 larvae (Fig. 1d). As the *let-7* transgene does not contain the *let-7* promoter, this regulation must occur post-transcriptionally. In addition to the qualitative analysis of fluorescent protein expression using microscopy we quantified the activity of the *let-7 sensor* using flow cytometry of whole animals. We used a COPAS Biosort instrument to quantify GFP and mCherry expression along the body axis of thousands of individual animals at different stages during development. *let-7 sensor* silencing was least efficient at the L1 larval stage, and reached maximal efficiency during L3 (Supplementary Methods and Supplementary Fig. 1). This correlates with the temporal expression pattern of *let-7*, which begins to accumulate during the L3 stage²¹. Since *let-7* is being driven by a promoter active at all stages, but appears active only at later larval stages, these data may reflect a mechanism that post-transcriptionally regulates *let-7* during development.

LIN-28 regulates pre-*let-7* processing

Next we carried out forward genetic and RNAi screens to identify factors regulating *let-7* activity *in vivo*. Knockdown of *lin-28* by RNAi resulted in reduced GFP at L1 and L2 stages, in a manner dependent on the *myo-2::let-7* transgene (Supplementary Fig. 2a,b and data not shown). We confirmed these results using a *lin-28* loss-of-function mutant (Fig. 1e and data not shown). Mutations in *lin-46* completely suppress the developmental timing defect of *lin-28* mutants²², but do not restore developmental regulation of *let-7* (Fig. 1e). Thus deregulation of *let-7* activity in *lin-28* mutants is not an indirect consequence of developmental timing defects. Other heterochronic genes, including *lin-14* and *lin-42* did not affect the *let-7 sensor* (Supplementary Fig. 2c and data not shown). Next we tested if LIN-28 was sufficient to inhibit *let-7* activity. Ectopic expression of LIN-28 in the pharynx from an extrachromosomal array resulted in inhibition of *let-7* in adults, which do not normally express LIN-28⁸ (Fig. 1f). Mosaic expression of the extrachromosomal array within the pharynx indicated that LIN-28 acts cell autonomously. We concluded that LIN-28 is required and sufficient to inhibit *let-7* activity in *C. elegans*.

We then used miRNA microarrays and northern blotting to confirm that LIN-28 regulates endogenous *let-7* accumulation in L2 larvae (Supplementary Data 1; Supplementary Fig. 3)²³. Further, expression of other *let-7* family members was not increased in *lin-28* mutants, whereas three unrelated miRNAs, including the developmentally regulated miRNA miR-85, showed increased expression in *lin-28* mutant L2s (Supplementary Fig. 3a,b).

Whether Lin28 regulates *let-7* processing at the Drosha^{15,16} or Dicer^{17,18} step in mammalian cells is unresolved. We addressed this *in vivo* in *C. elegans*. We used northern blotting and qRT-PCR to compare expression of *let-7* and its processing intermediates from the *myo-2::let-7* transgene in otherwise wild-type and *lin-28* mutant L2 larvae. *lin-28* mutants expressed higher levels of *let-7* compared to wild type, indicating increased processing efficiency; this was accompanied by a slight reduction in the level of pre-*let-7*, and no change in pri-*let-7* levels; these data are consistent with increased efficiency of Dicer-mediated processing (Supplementary Fig. 3c,d). We obtained similar results for endogenous *let-7*, although levels of pri-*let-7* were decreased in *lin-28* mutants, suggesting an indirect effect on the *let-7* promoter (Supplementary Fig. 3e,f). Interestingly, miR-85 also appears to be regulated at the Dicer step in a *lin-28*-dependent fashion (Supplementary Fig. 3b,g). Consistent with these findings a functional LIN-28-GFP translational fusion is localised in the cytoplasm⁸ (Supplementary Fig. 4a and data not shown). Taken together, these data suggest that LIN-28 blocks Dicer-mediated processing of *let-7* and possibly other developmentally regulated miRNAs.

Next, we tested whether LIN-28 directly interacts with pre-*let-7*. We performed pull-down assays using streptavidin beads and biotinylated pre-*let-7*. LIN-28-GFP from transgenic worm extracts was retained on streptavidin beads if the synthetic pre-*let-7* RNA was biotinylated, but not using a non-biotinylated control (Supplementary Fig. 4b). We tested whether this interaction was direct by native gel mobility shift assay. pre-*let-7* and GST-LIN-28 interact with an estimated K_d of 2 μ M (Supplementary Fig. 4c and data not shown). We conclude that LIN-28 binds pre-*let-7* to prevent Dicer processing. Experiments in mammalian cells suggested that the loop of the pre-*let-7* hairpin is required for the interaction with Lin28^{15,24}. However, the pre-*let-7* loop is not conserved in *C. elegans*. We therefore tested a number of pre-*let-7* loop mutants *in vivo* using the *let-7* sensor. We found that the pre-*let-7* loop is not required for the normal developmental regulation of *let-7* activity (see Supplementary Methods and Supplementary Fig. 5).

PUP-2 regulates pre-*let-7* processing in a *lin-28* dependent fashion

Our results so far were consistent with a LIN-28 blockade of pre-*let-7* processing, but we were puzzled that pre-*let-7* accumulation in L2 larvae differed little in wild-type compared to *lin-28* mutant animals (Supplementary Fig. 3). We reasoned that LIN-28 might target pre-*let-7* for degradation. Recent work by Kim and colleagues demonstrated that Lin28 promotes pre-*let-7* uridylation and subsequent degradation in mammalian cell lines, although the enzyme(s) involved are unknown¹⁸. We inspected published high-throughput sequencing data of *C. elegans* small RNA libraries^{25,26}, and found frequent modification of the 3' end of *let-7** with 1 or 2 untemplated uracil residues (*C. elegans let-7* resides on the 5' arm of the hairpin; Fig. 2a). These species are likely to arise from Dicer processing of partially uridylated intermediates, and indicate *in vivo* uridylation of *let-7*. Therefore we carried out an RNAi screen against 15 potential poly(U) polymerases (Supplementary Table 1) assaying *let-7* and pre-*let-7* abundance in *myo-2::let-7* transgenic L2 larvae. RNAi against *pup-2* resulted in increased pre-*let-7* levels (Fig. 2b,c; $P = 7.5 \times 10^{-5}$), and a small but significant increase in mature *let-7* levels (Fig. 2b,d; $P = 0.029$). This effect is specific to *pup-2*, no other poly(U) polymerases, including *cid-1*, a potential paralogue, had this effect²⁷ (Fig. 2c,d). These data suggest that PUP-2 uridylation targets pre-*let-7* for degradation, and is required for maximally efficient blockade of *let-7* processing by LIN-28.

We reasoned that LIN-28 might target uridylation of pre-*let-7* by PUP-2, leading to degradation of the uridylated pre-*let-7* and turnover of LIN-28/pre-*let-7* complexes, ensuring efficient LIN-28 function. We examined the effect of *pup-2* RNAi in situations where pre-*let-7* is released from LIN-28 blockade. The effect of *pup-2* RNAi on pre- and mature *let-7* levels is abolished at the L4 stage (Fig. 2c,d $P = 1 \times 10^{-5}$ and $P = 0.01$ respectively). Further, L2 larvae exposed to both *pup-2* and *lin-28* RNAi show significantly reduced accumulation of pre-*let-7* (Fig. 2c $P = 0.0003$). These effects are not due to reduced RNAi against *pup-2* (Supplementary Fig. 6a). In contrast, the effect of *lin-28* RNAi on mature *let-7* levels is not altered in *lin-28*, *pup-2* double RNAi L2 larvae (Fig. 2d $P = 0.2$). From these data we concluded that PUP-2 post-transcriptionally regulates *let-7* in a LIN-28-dependent fashion.

PUP-2 contributes to LIN-28-dependent regulation of *let-7* during development

Next we sought to determine if PUP-2 is required for regulation of *let-7* during development. Misregulation of *let-7* results in altered timing of larval development, defects in differentiation of a hypodermal stem cell lineage required for the formation of adult-specific lateral alae⁴, and defects in vulval morphogenesis²¹. Lateral seam cells differentiate and fuse into a syncytium in wild-type adults, but this fusion is defective if *pup-2* or *lin-28* is knocked down, consistent with a role in regulating *let-7* (Fig. 2e, Supplementary Table 2). *pup-2* RNAi in a *lin-28* null mutant background does not increase seam cell fusion defects suggesting this activity of *pup-2* is *lin-28* dependent (Table 1). Next we tested whether *pup-2* genetically interacts with *let-7*. *let-7(n2853ts)* animals show reduced *let-7* expression and temperature sensitive vulval bursting²¹. At 15°C, vulval bursting of *let-7(n2853ts)* animals was suppressed by *pup-2* RNAi, whereas *lin-28* RNAi suppressed vulval bursting at both 15°C and 20°C (Table 1). Weaker suppression of *let-7(n2853ts)* by *pup-2* compared to *lin-28* is consistent with a role for *pup-2* as a *lin-28* modifier. Taken together with the effect of *pup-2* on *let-7* processing, these data indicate *pup-2* ensures efficient activity of *lin-28* by targeting blocked pre-*let-7* molecules for destruction. This might occur via LIN-28 dependent uridylyl-transferase activity of PUP-2 on pre-*let-7*; we sought to test this hypothesis *in vitro*.

PUP-2 uridylates pre-*let-7* in a LIN-28 dependent fashion *in vitro*

We expressed HA-FLAG tagged PUP-2 and SBP tagged LIN-28 in a HEK293T human embryonic kidney cell line. Immunoprecipitation of HA-FLAG-PUP2 using anti-FLAG antibodies specifically co-precipitated SBP-LIN-28 (Fig. 3a). This interaction was in absence of *C. elegans* pre-*let-7* and likely direct. Indeed, the addition of excess exogenous pre-*let-7* to the cell extract did not enhance the interaction. We also confirmed this interaction in GST pull-down experiments. *In vitro* translated PUP-2 directly interacts with GST-LIN-28 (Fig. 3b). PUP-2 was previously shown to polyuridylate an artificially tethered RNA in *Xenopus* oocytes, but was inactive without tethering²⁷. Therefore, we tested if LIN-28 might be able to recruit PUP-2 to mediate pre-*let-7* uridylation (Fig. 3c). We incubated anti-FLAG immunoprecipitates from cell extracts expressing HA-FLAG-PUP2 and/or SBP-LIN-28 with radiolabeled pre-*let-7* and radiolabelled UTP. We find that HA-FLAG-PUP2 uridylated pre-*let-7* only in the presence of SBP-LIN-28 (Fig. 3c). We also confirmed LIN-28 dependent uridylation of pre-*let-7* by PUP-2 *in vitro* (Supplementary Fig. 6b). Finally, we attempted to identify *in vivo* uridylated pre-*let-7* directly by cloning, but we were unable to do so. We conclude that rapid degradation of uridylated pre-*let-7* prevents accumulation of these species *in vivo*, as has been postulated in human cell lines¹⁸.

DISCUSSION

We have developed a quantitative assay of *let-7* miRNA function in *C. elegans*. This assay is highly sensitive and amenable to high-throughput experiments. We have isolated new mutants in known miRNA pathway components through mutagenesis screens using this assay; analysis of novel miRNA function defective mutants should provide insights into the miRNA mechanism. In addition, this assay could be modified to study post-transcriptional regulation or target specificity of other miRNAs.

Here we demonstrate that LIN-28 regulates *C. elegans* pre-*let-7* (see Supplementary Fig. 7a for a model). These results provide a molecular basis for the genetic link between *lin-28* and *let-7* in controlling developmental timing. In *C. elegans* this pathway determines the behaviour of epithelial stem cells. In mammals *let-7* and Lin28 might regulate primordial germ cell differentiation and other stem cell lineages²⁸. Therefore, the specific interaction of a structured RNA (pre-*let-7*) with a protein (Lin28) constitutes an ultraconserved switch regulating stem cell differentiation. The *let-7*/lin-28 switch might be as conserved as *let-7* itself. For example, pre-*let-7* processing is developmentally regulated in the sea urchin *Strongylocentrotus purpuratus*¹³, which also expresses a Lin28 orthologue (data not shown).

Our finding that the terminal loop of pre-*let-7* is dispensable for regulation by LIN-28 is at odds with two previous studies^{15,16}, but is consistent with competition experiments carried out by Rybak *et al.*¹⁷. Our approach has been to assess *let-7* function *in vivo*, whereas previous work was based on *in vitro* interaction studies. All 22 nucleotides of mature *let-7* are conserved in bilateria, whereas for many other miRNAs only the “seed” sequence (nucleotides 2 to 8) appears to be under evolutionary constraint. In contrast, there is little sequence similarity in the terminal loops of *let-7* in different species. It is therefore tempting to speculate that nucleotides corresponding to mature *let-7* contribute to LIN-28 recognition. Similar RNA-protein interactions might impose evolutionary constraint on the sequences of other ultraconserved miRNAs.

Here we show that LIN-28 recruits the poly(U) polymerase PUP-2 to uridylylate *C. elegans* pre-*let-7*. We speculate that mammalian PUP-2 orthologues might similarly regulate *let-7* in stem cells (Supplementary Fig. 7b). Indeed, the mouse Tut4/Zcchc11 uridylyl transferase regulates *let-7* in embryonic stem cells²⁹. *let-7* is a candidate tumour suppressor^{21,30,31,32} and LIN28 is a potential proto-oncoprotein^{28,33}. Therefore TUT4/ZCCHC11 might be an important novel target for anti-cancer therapy. Our data suggest that miRNAs are regulated through pre-miRNA sequestration and uridylation-dependent pre-miRNA degradation. This situation appears to be analogous to two-step regulation of the activity of proteins through sequestration and targeted degradation, for example in the case of cadherin³⁴. Uridylation-dependent degradation of RNA has been observed previously and U tails have been shown to recruit either 5' to 3' or 3' to 5' exonucleases^{35,36}. High-throughput sequencing suggests additional miRNAs and/or pre-miRNAs are subject to uridylation (data not shown), so regulation in this way may be widespread. Further uncovering the mechanisms underlying this pathway will be of great interest.

Supplementary Material

Refer to Web version on PubMed Central for supplementary material.

Acknowledgments

We thank Andrea Hutterer (Wellcome Trust Cancer Research UK Gurdon Institute, University of Cambridge, Cambridge, UK) for a strain carrying the *mjls15* transgene, Mark Jackman (Wellcome Trust Cancer Research UK Gurdon Institute, University of Cambridge, Cambridge, UK) for pDEST-MAL, pcDNA5/FRT/

TO_GATEWAY_TEV_SBP and pDEST-3FLAG 3HA vectors, Eric Moss (University of Medicine and Dentistry of New Jersey, NJ) for anti-LIN-28 antibody, and Marv Wickens (Department of Biochemistry, University of Wisconsin, MA) for PUP-2 cDNA. We thank Richard Gregory and Narry Kim for sharing unpublished data. N.J.L. and K.J.M. were supported by a PhD studentship from the Wellcome Trust (UK). J.A. and A.B. were supported by grants from the Biotechnology and Biological Sciences Research Council (UK). H.L.L. was supported by a PhD studentship from Cancer Research UK. This work was supported by a Cancer Research UK Programme Grants to E.A.M. and S.B. and core funding to the Wellcome Trust/Cancer Research UK Gurdon Institute provided by the Wellcome Trust and Cancer Research UK.

Appendix

Online Methods

Nematode culture and strains

We grew *C. elegans* under standard conditions at 20 °C³⁷. The food source used was *E. coli* strain HB101 (*Caenorhabditis* Genetics Center, University of Minnesota, Twin Cities, MN, USA). We used bleaching followed by starvation-induced L1 arrest to generate synchronized cultures. The wild-type strain was var. Bristol N2³⁸. Additional strains used are listed in Supplementary Table 3.

DNA constructs and transgenics

We generated DNA vectors using the Multisite Gateway Three-Fragment vector construction kit (Invitrogen; Supplementary Data 2). We performed site directed mutagenesis using PCR and mutagenic primers (Supplementary Data 2). All constructs were confirmed by sequencing. To generate transgenic animals, we performed germline transformations as described³⁹. Injection mixes contained 2-10 ng μl^{-1} of vector, 5-10 ng μl^{-1} of marker, and Invitrogen 1 kb ladder to a final concentration of 100 ng μl^{-1} DNA (see Supplementary Methods for details). We integrated array transgenes via X-ray irradiation as described⁴⁰. We generated single copy transgenes by transposase mediated integration (mosSCI) as described⁴¹.

Microscopy

We carried out differential interference contrast (DIC) and fluorescence imaging using standard methods⁴² and using an AxioImager A1 upright microscope (Zeiss, Jena, Germany). We captured images using an ORCA-ER digital camera (Hamamatsu, Hamamatsu, Japan) and processed images using OpenLabs 4.0 software (Improvision, Coventry, UK). For analysis of *let-7 sensor* transgene expression, we imaged all animals under identical conditions. We performed confocal microscopy using an Olympus FluoView FV1000 upright microscope using 63x objective magnification.

Analyses with the COPAS Biosort instrument

We used a COPAS Biosort instrument (Union Biometrica, Holliston, MA, USA) to simultaneously measure length (time of flight), absorbance (extinction), and fluorescence. We optimized fluorophore detection for simultaneous detection of GFP and mCherry. We used a multiline solid state argon laser for excitation (488nm GFP and 561nm mCherry), and detected emission by appropriate PMTs after passing through band pass filters (510/23nm GFP and 615/45nm mCherry). We harvested animals from plates and washed in M9 buffer³⁷ prior to sorting. We determined length and absorbance for each larval stage using synchronised wild-type populations. We then generated gates to isolate animals of specific developmental stages from mixed populations (Supplementary Fig. 1a).

RNA interference assays

We obtained RNAi clones from genome-wide RNAi libraries^{43,44,45}. We generated additional RNAi constructs by subcloning of an appropriate genomic DNA fragment into pDEST-L4440^{45,46} (Supplementary Data 2). We confirmed all RNAi constructs by sequencing. For experiments using *let-7 sensor* and *myo-2::let-7* transgenes we performed RNAi by feeding as described using the *eri-1(mg366)* RNAi hypersensitive genetic background⁴⁷. For COPAS Biosort analysis, we plated 10-50 L1 larvae on 90 mm RNAi plates, and analysed animals once the oldest progeny reached the L3 larval stage. For harvest and RNA extraction we plated ~3,000 L1 larvae per RNAi plate and grew animals to adulthood prior to bleaching. After synchronisation by starvation, we plated the progeny onto fresh RNAi plates and grew to the desired stage before harvesting. We performed RNAi by injection as described⁴⁸. We analyzed phenotypes on progeny laid 24-48 hrs post-injection.

Phenotypic analysis of seam cell development

We performed RNAi by injection into strains carrying seam cell marker transgenes *wIs51* and *mjIs15*.

Vulval bursting assay

let-7(n2853ts) embryos were added to RNAi plates by bleaching gravid adults, and grown at 15 °C. Non-burst adults were then transferred to fresh RNAi plates and temperature-shifted as required. L4 progeny were picked to fresh RNAi plates (15-25 animals per plate), and vulval bursting was scored after 48 hrs.

RNA Extraction

For total RNA isolation we harvested animals from plates by washing with M9³⁷. We pelleted and froze animals in liquid nitrogen and dissolved pellets in 10 volumes of Trizol reagent (Invitrogen, Carlsbad, CA, USA). We extracted total RNA from Trizol reagent according to the manufacturer's protocol.

miRNA microarray analysis

We performed miRNA microarrays using custom DNA oligonucleotide arrays as described previously^{49,50}. Data analysis was as described⁵⁰. To compare miRNA expression in wild-type and *lin-28* mutant L2 larvae we isolated and size selected total RNA from synchronized animals to 18-26 nt using polyacrylamide gel electrophoresis. The small RNA fraction was 3' end-labelled using T4 RNA ligase (Fermentas UK, York, UK). *C. elegans* miRNA microarrays were based on miRbase release 8.0^{51,52}. We performed all experiments in triplicates. For microarray probe information and primary microarray data see Supplementary Data 1.

Northern blotting

We performed northern blotting as described^{25,53}, with the following modifications. We used 5-20 µg total RNA, or small RNA fraction (miRvana, Ambion) isolated from ~200 µg total RNA. For developmental expression profiles (Supplementary Fig. 3a) we carried out 1-ethyl-3-[3-dimethylaminopropyl]carbodiimide hydrochloride (EDC, Perbio Science, Erembodegem, Belgium) crosslinking reactions for 2 hrs at 60 °C. Otherwise blots were UV-crosslinked. We modified northern hybridisations as follows; membranes were pre-hybridised at 40 °C for 4 hrs in hybridisation buffer (0.36 M Na₂HPO₄, 0.14 M NaH₂PO₄, 7% (v/v) SDS and 1 mg of sheared, denatured salmon sperm DNA) and hybridised at 40 °C overnight using 20 pmole of γ-³²P-ATP-radiolabelled DNA oligonucleotide probes (Supplementary Data 2). After hybridisation, we washed membranes twice with 0.5 xSSC,

0.1 % (v/v) SDS at 40 °C for 10 min and once with 0.1 xSSC, 0.1 % (v/v) SDS at 40 °C for 5min. We detected radioactivity by phosphoimager (GE Healthcare, Amersham, UK). We quantified band intensity using ImageQuant software (GE Healthcare).

Real-time RT-PCR

We performed RT-PCR as described²⁵, using the standard curve method. Primers used are listed in Supplementary Data 2.

pre-*let-7* pull-down

For these experiments we generated a strain carrying a rescuing *lin-28::gfp* translational fusion transgene (mosSCI integrated) in a *lin-28(n719)* mutant background. We prepared protein extracts from starvation synchronised L1 larvae. We cleared lysates against streptavidin Dynabeads (Invitrogen) for 30 min at 4 °C in PD buffer [18 mM HEPES-KOH pH 7.9, 10 % (v/v) glycerol, 40 mM KCl, 2 mM MgCl₂, 10 mM DTT, 100 μM ZnSO₄, 1x Proteinase Inhibitor Cocktail (PIC; Roche)]. Dynabeads were blocked with 15 μg yeast tRNA for 1 h at 4 °C in PD buffer before addition of 100 pmol synthetic 5' biotinylated pre-*let-7* (Microsynth, Balgach, Switzerland) for pull-down, or unmodified synthetic pre-*let-7* for control reactions, and incubated for 1 hr at room temperature. We added pre-blocked Dynabeads to the binding reaction and incubated for 1 h at room temperature. We washed beads 3 times in PD buffer. We analyzed bound proteins by western blotting with primary mouse anti-GFP (Clontech JL-8; 1:1000) and secondary HRP-conjugated anti-mouse (Dakocytomation P0450; 1:10,000), or rat anti-tubulin (Chemicon international MAB1684, 1:1000) and secondary HRP-conjugated mouse anti-rat (GE Healthcare NA9310; 1:10,000).

Recombinant protein expression

We obtained LIN-28 cDNA (F02E9.2b) from the ORFeome library⁴⁵. We subcloned cDNAs into pDEST-GEX-2TK (Gateway cassette inserted at SmaI site in pGEX-2TK), or pDEST-MAL. We expressed and purified recombinant proteins as described^{25,54}.

GST-pull-down

We used PUP-2 cDNA in pDEST14 (Invitrogen) to produce ³⁵S-methionine-radiolabelled protein by *in vitro* transcription-translation using a TNT T7 coupled reticulocyte lysate kit (Promega). We performed pull-downs were performed using GST-LIN-28 as described⁵⁴.

Pre-*let-7* transcription

We performed *in vitro* transcription reactions in a volume of 20 μl with 0.5 mM of each NTP, 40 mM Tris pH 7.9, 12 mM MgCl₂, 2 mM spermidine, 20 mM DTT, 1 mM NaCl, 100 U T7 RNA polymerase (Roche, Basel, Switzerland), and 1U RNasin (Promega, Madison WI, USA). We incubated reactions for 1 hr at 37 °C, prior to phenol/chloroform extraction and ethanol precipitation. We transcribed radiolabeled RNA for electrophoretic mobility shift assays with α-³²P-UTP to a specific activity of approximately 6,000 cpm/fmol.

Immunoprecipitation

We cloned LIN-28 cDNA into pcDNA5/FRT/TO_GATEWAY_TEV_SBP. We cloned PUP-2 cDNA into pDEST-3FLAG 3HA. We performed immunoprecipitation assays as described previously¹⁸. Briefly, we transfected HEK293T cells with pHA-FLAG-PUP-2 and/or pLIN-28-SBP. After 48h we collected cells in cold lysis buffer (500mM NaCl, 1mM EDTA, 10 mMTris (pH8.0), 1% (v/v) Triton X-100), sonicated for 4 min on ice and centrifugated for 10 min. We incubated 50 μl of the supernatant was with 5 μl of pre-washed anti-FLAG antibody, conjugated to agarose beads (Sigma) and incubated for 2 hr at 4°C. We washed agarose-beads twice with lysis buffer and twice with buffer D. For *in vitro*

uridylation, we incubated agarose beads in a 30 μ l reaction containing 3.2 mM of MgCl₂, 1 mM of DTT and 0.25 mM of rUTP and 5'-end-labeled pre-miRNA of 1×10^4 - 1×10^5 cpm, for 20 min at 37 °C. We purified RNA by Trizol extraction and isopropanol precipitation. We analyzed reactions in a 12% urea polyacrylamide gel.

***In vitro* uridylation assays**

We performed *in vitro* uridylation assays in 30 μ l reactions containing 1.5 μ g of *in vitro* transcribed pre-*let-7* in 10 mM Tris pH 7.5, 30 mM KCl, 1 mM DTT, 10 mM MnCl₂, 2 mM MgCl₂, 0.25 mM UTP, 1 μ l of RNaseOut and 0.01 Mbq α -³²P-UTP. We added 1 μ g of recombinant MBP-PUP-2 and increasing amounts of recombinant GST-LIN-28 to a maximum of 10 μ g. We incubated reaction mixtures at 30 °C for 30 min. We purified RNA by phenol/chloroform extraction and ethanol precipitation. We analyzed reactions in a 6% urea polyacrylamide gel. We used 2U of *S. pombe* CID1 poly(U) polymerase (NEB, Ipswich, MA, USA) as a positive control. We detected radioactivity by phosphoimager (GE Healthcare).

Electrophoretic mobility shift assay

We carried out binding reactions in a total volume of 20 μ l containing 50,000 cpm of radiolabelled RNA, 30 μ g tRNA, 1 μ l RNaseOut (40 unit/ μ l, Invitrogen), 50 mM Tris pH 7.6, 100 mM NaCl, 0.07 % (v/v) β -mercaptoethanol, 5 mM MgOAc₂, and increasing amounts of recombinant GST-LIN-28 to a maximum of 10 μ M. We incubated the reactions at room temperature for 45 min, followed by analysis using 5% native polyacrylamide gel electrophoresis. We detected radioactivity by phosphoimager (GE Healthcare).

References

1. Bartel DP. MicroRNAs: genomics, biogenesis, mechanism, and function. *Cell*. 2004; 116:281–297. [PubMed: 14744438]
2. Bartel DP. MicroRNAs: target recognition and regulatory functions. *Cell*. 2009; 136:215–233. [PubMed: 19167326]
3. Kim VN, Han J, Siomi MC. Biogenesis of small RNAs in animals. *Nat Rev Mol Cell Biol*. 2009; 10:126–139. [PubMed: 19165215]
4. Ambros V, Horvitz HR. Heterochronic mutants of the nematode *Caenorhabditis elegans*. *Science*. 1984; 226:409–416. [PubMed: 6494891]
5. Chalfie M, Horvitz HR, Sulston JE. Mutations that lead to reiterations in the cell lineages of *C. elegans*. *Cell*. 1981; 24:59–69. [PubMed: 7237544]
6. Lee RC, Feinbaum RL, Ambros V. The *C. elegans* heterochronic gene *lin-4* encodes small RNAs with antisense complementarity to *lin-14*. *Cell*. 1993; 75:843–854. [PubMed: 8252621]
7. Wightman B, Ha I, Ruvkun G. Posttranscriptional regulation of the heterochronic gene *lin-14* by *lin-4* mediates temporal pattern formation in *C. elegans*. *Cell*. 1993; 75:855–862. [PubMed: 8252622]
8. Moss EG, Lee RC, Ambros V. The cold shock domain protein LIN-28 controls developmental timing in *C. elegans* and is regulated by the *lin-4* RNA. *Cell*. 1997; 88:637–646. [PubMed: 9054503]
9. Slack FJ, et al. The *lin-41* RBCC gene acts in the *C. elegans* heterochronic pathway between the *let-7* regulatory RNA and the LIN-29 transcription factor. *Mol Cell*. 2000; 5:659–669. [PubMed: 10882102]
10. Abrahante JE, et al. The *Caenorhabditis elegans* hunchback-like gene *lin-57/hbl-1* controls developmental time and is regulated by microRNAs. *Dev Cell*. 2003; 4:625–637. [PubMed: 12737799]
11. Grosshans H, Johnson T, Reinert KL, Gerstein M, Slack FJ. The temporal patterning microRNA *let-7* regulates several transcription factors at the larval to adult transition in *C. elegans*. *Dev Cell*. 2005; 8:321–330. [PubMed: 15737928]

12. Lin SY, et al. The *C. elegans* hunchback homolog, *hbl-1*, controls temporal patterning and is a probable microRNA target. *Dev Cell*. 2003; 4:639–650. [PubMed: 12737800]
13. Pasquinelli AE, et al. Conservation of the sequence and temporal expression of *let-7* heterochronic regulatory RNA. *Nature*. 2000; 408:86–89. [PubMed: 11081512]
14. Winter J, Jung S, Keller S, Gregory RI, Diederichs S. Many roads to maturity: microRNA biogenesis pathways and their regulation. *Nat Cell Biol*. 2009; 11:228–234. [PubMed: 19255566]
15. Newman MA, Thomson JM, Hammond SM. Lin-28 interaction with the *Let-7* precursor loop mediates regulated microRNA processing. *RNA*. 2008; 14:1539–1549. [PubMed: 18566191]
16. Viswanathan SR, Daley GQ, Gregory RI. Selective blockade of microRNA processing by Lin28. *Science*. 2008; 320:97–100. [PubMed: 18292307]
17. Rybak A, et al. A feedback loop comprising *lin-28* and *let-7* controls pre-*let-7* maturation during neural stem-cell commitment. *Nat Cell Biol*. 2008; 10:987–993. [PubMed: 18604195]
18. Heo I, et al. Lin28 mediates the terminal uridylation of *let-7* precursor MicroRNA. *Mol Cell*. 2008; 32:276–284. [PubMed: 18951094]
19. Yu J, et al. Induced pluripotent stem cell lines derived from human somatic cells. *Science*. 2007; 318:1917–1920. [PubMed: 18029452]
20. Miller DM, Stockdale FE, Karn J. Immunological identification of the genes encoding the four myosin heavy chain isoforms of *Caenorhabditis elegans*. *Proc Natl Acad Sci USA*. 1986; 83:2305–2309. [PubMed: 2422655]
21. Reinhart BJ, et al. The 21-nucleotide *let-7* RNA regulates developmental timing in *Caenorhabditis elegans*. *Nature*. 2000; 403:901–906. [PubMed: 10706289]
22. Pepper AS, et al. The *C. elegans* heterochronic gene *lin-46* affects developmental timing at two larval stages and encodes a relative of the scaffolding protein gephyrin. *Development*. 2004; 131:2049–2059. [PubMed: 15073154]
23. Bracht J, Hunter S, Eachus R, Weeks P, Pasquinelli AE. Trans-splicing and polyadenylation of *let-7* microRNA primary transcripts. *RNA*. 2004; 10:1586–1594. [PubMed: 15337850]
24. Piskounova E, et al. Determinants of microRNA processing inhibition by the developmentally regulated RNA-binding protein Lin28. *J Biol Chem*. 2008; 283:21310–21314. [PubMed: 18550544]
25. Das PP, et al. Piwi and piRNAs act upstream of an endogenous siRNA pathway to suppress Tc3 transposon mobility in the *Caenorhabditis elegans* germline. *Mol Cell*. 2008; 31:79–90. [PubMed: 18571451]
26. Batista PJ, et al. PRG-1 and 21U-RNAs interact to form the piRNA complex required for fertility in *C. elegans*. *Mol Cell*. 2008; 31:67–78. [PubMed: 18571452]
27. Kwak JE, Wickens M. A family of poly(U) polymerases. *RNA*. 2007; 13:860–867. [PubMed: 17449726]
28. West JA, et al. A role for Lin28 in primordial germ-cell development and germ-cell malignancy. *Nature*. 2009
29. Gregory RI. Lin28 recruits the TUTase Zcchc11 to inhibit *let-7* maturation in embryonic stem cells. *Nat Struct Mol Biol*. 2009
30. Johnson CD, et al. The *let-7* microRNA represses cell proliferation pathways in human cells. *Cancer Res*. 2007; 67:7713–7722. [PubMed: 17699775]
31. Johnson SM, et al. RAS is regulated by the *let-7* microRNA family. *Cell*. 2005; 120:635–647. [PubMed: 15766527]
32. Yu F, et al. *let-7* regulates self renewal and tumorigenicity of breast cancer cells. *Cell*. 2007; 131:1109–1123. [PubMed: 18083101]
33. Chang TC, et al. Lin-28B transactivation is necessary for Myc-mediated *let-7* repression and proliferation. *Proc Natl Acad Sci USA*. 2009; 106:3384–3389. [PubMed: 19211792]
34. Kowalczyk AP, Reynolds AB. Protecting your tail: regulation of cadherin degradation by p120-catenin. *Curr Opin Cell Biol*. 2004; 16:522–527. [PubMed: 15363802]
35. Mullen TE, Marzluff WF. Degradation of histone mRNA requires oligouridylation followed by decapping and simultaneous degradation of the mRNA both 5′ to 3′ and 3′ to 5′. *Genes Dev*. 2008; 22:50–65. [PubMed: 18172165]

36. Rissland OS, Norbury CJ. Decapping is preceded by 3' uridylation in a novel pathway of bulk mRNA turnover. *Nat Struct Mol Biol.* 2009
37. Wood, W. *The Nematode Caenorhabditis elegans.* Cold Spring Harbour Press; 1988.
38. Brenner S. The genetics of *Caenorhabditis elegans.* *Genetics.* 1974; 77:71–94. [PubMed: 4366476]
39. Mello C, Fire A. DNA transformation. *Methods Cell Biol.* 1995; 48:451–482. [PubMed: 8531738]
40. Fire A. Integrative transformation of *Caenorhabditis elegans.* *EMBO J.* 1986; 5:2673–2680. [PubMed: 16453714]
41. Frøkjaer-Jensen C, et al. Single-copy insertion of transgenes in *Caenorhabditis elegans.* *Nat Genet.* 2008; 40:1375–1383. [PubMed: 18953339]
42. Horvitz HR, Sulston JE. Isolation and genetic characterization of cell-lineage mutants of the nematode *Caenorhabditis elegans.* *Genetics.* 1980; 96:435–454. [PubMed: 7262539]
43. Fraser AG, et al. Functional genomic analysis of *C. elegans* chromosome I by systematic RNA interference. *Nature.* 2000; 408:325–330. [PubMed: 11099033]
44. Kamath RS, et al. Systematic functional analysis of the *Caenorhabditis elegans* genome using RNAi. *Nature.* 2003; 421:231–237. [PubMed: 12529635]
45. Rual JF, et al. Toward improving *Caenorhabditis elegans* phenome mapping with an ORFeome-based RNAi library. *Genome Res.* 2004; 14:2162–2168. [PubMed: 15489339]
46. Timmons L, Court DL, Fire A. Ingestion of bacterially expressed dsRNAs can produce specific and potent genetic interference in *Caenorhabditis elegans.* *Gene.* 2001; 263:103–112. [PubMed: 11223248]
47. Kennedy S, Wang D, Ruvkun GA. conserved siRNA-degrading RNase negatively regulates RNA interference in *C. elegans.* *Nature.* 2004; 427:645–649. [PubMed: 14961122]
48. Fire A, et al. Potent and specific genetic interference by double-stranded RNA in *Caenorhabditis elegans.* *Nature.* 1998; 391:806–811. [PubMed: 9486653]
49. Miska EA, et al. Microarray analysis of microRNA expression in the developing mammalian brain. *Genome Biol.* 2004; 5:R68. [PubMed: 15345052]
50. Wienholds E, et al. MicroRNA expression in zebrafish embryonic development. *Science.* 2005; 309:310–311. [PubMed: 15919954]
51. Griffiths-Jones S. The microRNA Registry. *Nucleic Acids Res.* 2004; 32:D109–111. [PubMed: 14681370]
52. Griffiths-Jones S, Grocock RJ, van Dongen S, Bateman A, Enright AJ. miRBase: microRNA sequences, targets and gene nomenclature. *Nucleic Acids Res.* 2006; 34:D140–144. [PubMed: 16381832]
53. Pall GS, Hamilton AJ. Improved northern blot method for enhanced detection of small RNA. *Nat Protoc.* 2008; 3:1077–1084. [PubMed: 18536652]
54. Sapetschnig A, et al. Transcription factor Sp3 is silenced through SUMO modification by PIAS1. *EMBO J.* 2002; 21:5206–5215. [PubMed: 12356736]

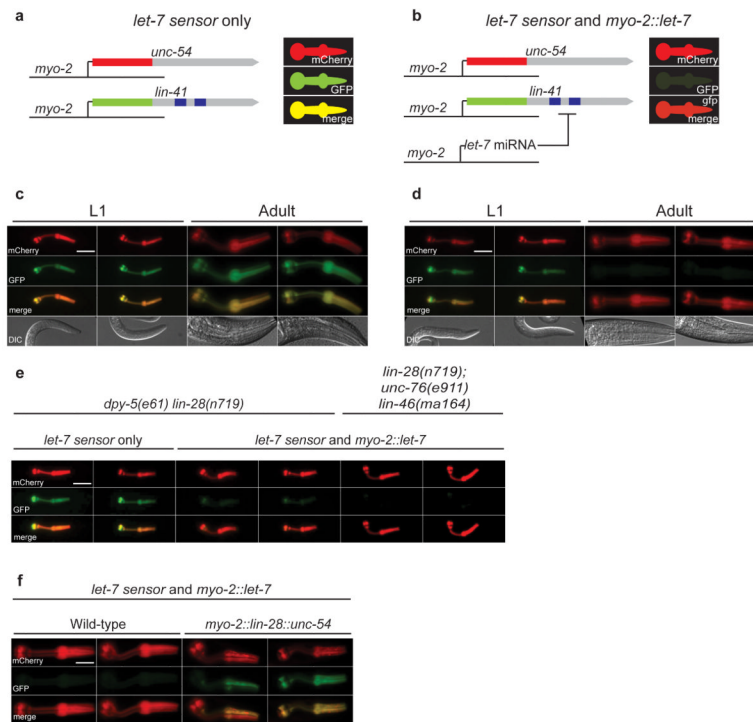


Figure 1. A quantitative assay reveals post-transcriptional regulation of the *let-7* miRNA by *lin-28*

(a,b) Schematic of the pharynx based assay of *let-7* activity. **(c)** Fluorescence images of animals carrying the *let-7 sensor* transgene at L1 larval and adult stages. Both GFP and mCherry are strongly expressed.

d Fluorescence images of animals carrying both the *let-7 sensor* and *myo-2::let-7* transgenes at L1 larval and adult stages. GFP is specifically and robustly downregulated in adults, but not in L1 larvae. Scale bar shows 20 μ m.

e Fluorescence images showing that *lin-28* mutants downregulate *let-7 sensor* GFP at the L1 stage in a *myo-2::let-7* dependent fashion. This effect is not reversed in a *lin-46* mutant background. Scale bar shows 20 μ m.

f Fluorescence images showing that a *myo-2::lin-28::unc-54* transgene is sufficient to block *let-7* activity in adults carrying *let-7 sensor* and *myo-2::let-7* transgenes. Scale bar shows 20 μ m.

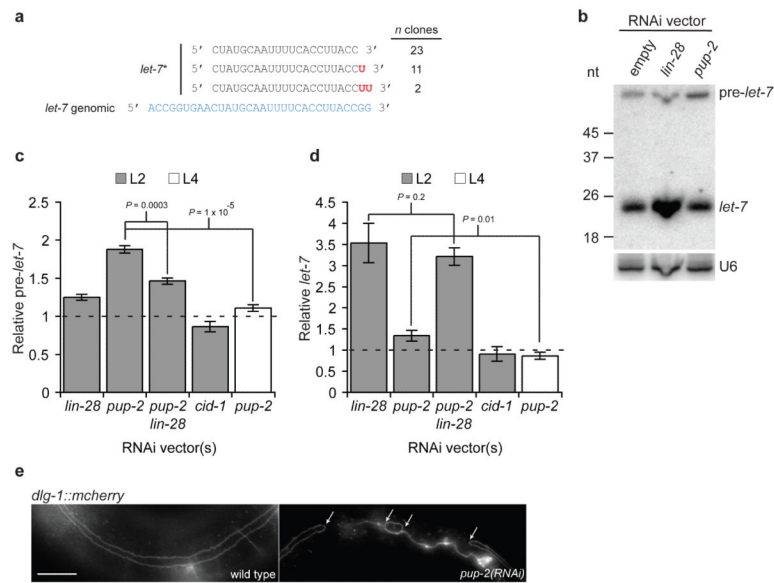


Figure 2. *pup-2* regulates *let-7* processing in a *lin-28*-dependent fashion

a *let-7* is uridylated *in vivo*. Frequency of unmodified and modified *let-7** molecules identified by high-throughput sequencing.

b Representative northern blot showing *pup-2*-dependent regulation of pre-*let-7*. 5 μ g of total RNA from control, *lin-28*(RNAi), and *pup-2*(RNAi) *myo-2::let-7*L2 larvae was loaded. U6 was used as a loading control.

c,d Quantification of relative pre-*let-7* (**c**), and *let-7* (**d**) abundance in *lin-28*(RNAi), *pup-2*(RNAi) and *cid-1*(RNAi) *myo-2::let-7*L2 and L4 larvae from northern blotting experiments. Mean fold change relative to empty vector control samples is shown. *P*-values from Student's *t*-tests indicated; *n* = 4. Error bars show standard error of the mean.

e Fluorescence image showing the seam cell defect observed in *pup-2*(RNAi) adults. A DLG-1-mCherry fusion marks seam cell boundaries. Upper panel; wild-type with continuous seam. Lower panel; *pup-2*(RNAi) with incompletely fused seam. Arrows indicate sites of failed fusion. Scale bar shows 20 μ m.

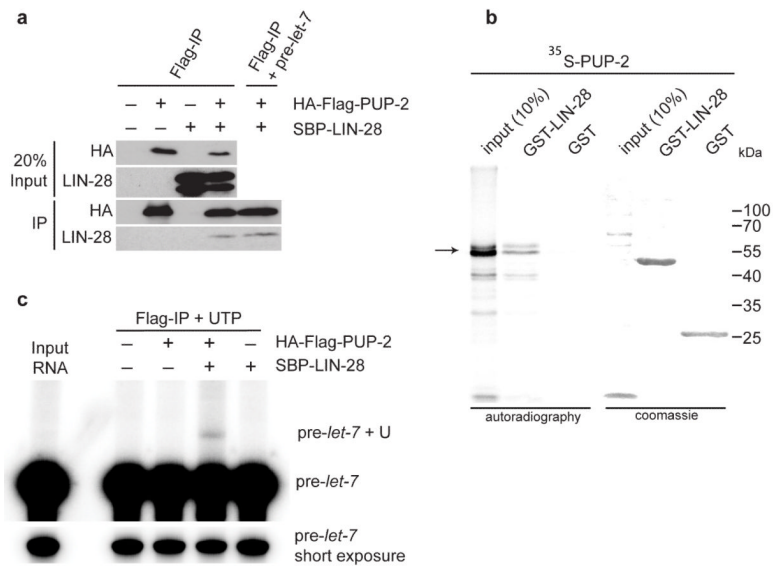


Figure 3. LIN-28 interacts with PUP-2 and promotes uridylation of pre-let-7 by PUP-2
a Co-Immunoprecipitation of PUP-2 and LIN-28 expressed in HEK293T cells.
b GST pull-down assay demonstrating a direct interaction of GST-LIN-28 and PUP-2 *in vitro*.
c *In vitro* uridylation assay showing that PUP-2 uridylates pre-let-7 in a LIN-28 dependent fashion.

Table 1Genetic interactions of *pup-2* and *lin-28* with *let-7* in vulval development

genotype	% burst at 20°C (n)	% burst at 15°C (n)
<i>let-7(n2853)</i> ; empty vector RNAi	97 (119)	47 (86)
<i>let-7(n2853)</i> ; <i>lin-28</i> (RNAi)	16 (115)	0 (28)
<i>let-7(n2853)</i> ; <i>pup-2</i> (RNAi)	97 (120)	28 (114)

RNAi by feeding.